The Abdus Salam
International Centre for Theoretical Physics

United Nations
Educational, Scientific and
Cultural Organization

IAEA
International Atomic Energy Agency

2055-13

Joint ICTP/IAEA School on Physics and Technology of Fast Reactors Systems

9 - 20 November 2009

Radiation Damage of Structural Materials

for Fast Reactor Fuel Assembly (2)

B. Raj & M. Vijayalakshmi
Indira Gandhi Centre for Atomic Research
India

RADIATION DAMAGE OF STRUCTURAL MATERIALS FOR FAST REACTOR FUEL ASSEMBLY

(ICTP/IAEA course, 9-20, Nov., 09, Trieste, Italy.)

BALDEV RAJ & M.VIJAYALAKSHMI

Indira Gandhi Centre for Atomic Research, KALPAKKAM-603 102, INDIA.

CONTENTS

S.N.	Title of Chapter
1.	**Introduction to structural materials and their behaviour in a fast reactor fuel assembly**
2.	Radiation Damage
3.	Principles of Design of Radiation Resistant Materials for Fast Reactor Fuel Assembly

CHAPTER 2

RADIATION DAMAGE

It has been shown in chapter.1 that the core components of a fast reactor fuel sub-assembly experience maximum radiation damage. The point defects, produced in two orders of magnitude excess of thermal equilibrium concentration, rearrange themselves into defect configurations, which lower the total energy of the system. These defects influence the physical and mechanical behaviour of materials and become finally the life limiting factors for the components in the nuclear reactor The details of the damage mechanisms, void swelling, irradiation growth, irradiation hardening, irradiation creep, embrittlement and helium embrittlement are discussed in this chapter.

VOID SWELLING:

Any component in a reactor has certain density of dislocations introduced in their lattice, due to industrial fabrication processes. These dislocations have a 'preferential bias' of around 2% towards interstitials than vacancies. This factor, called the 'dislocation bias' leads to locking up interstitials around the core of dislocations, leaving behind an excess concentration of vacancies, which do not find the required concentration of interstitials for 'recombination'. The excess concentration of vacancies, when exceeds the equilibrium concentration of vacancies, condenses into three dimensional defect clusters, forming the 'voids'. Figure.1. shows the schematic and micrograph of voids. These microscopic voids are responsible for the isotropic volume change (Figure.2.) in a core component material in a fast reactor fuel sub-assembly. The process is termed as 'void swelling', representing the volume change due to formation of voids. Void swelling which is one of the reasons for the dimensional change shown above, is measured in

terms of the ratio of increase in volume during irradiation to the original volume (∇V/V). This can be measured using change in density of bulk components of the reactor or image analysis of voids observed using transmission electron microscope. The extent of void swelling depends on material parameters like chemistry of the material and dislocation density and irradiation parameters like the dose, dose rate and nature of impinging particles. Presently, we have reached up to the stage of burn up of fuel around 10-12 at %. The target burn up is 20 at. %. The limiting factor for continuous increase in the burn-up of the fuel is the life of the clad material and not the fuel *per se* !!!

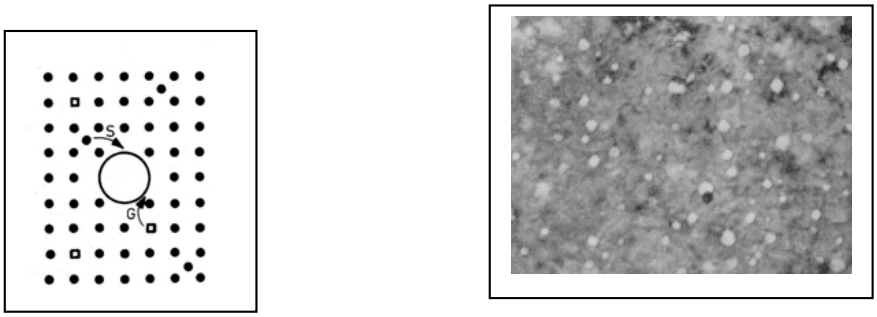

Figure.1.Schematic and electron micrograph of voids in a crystal.

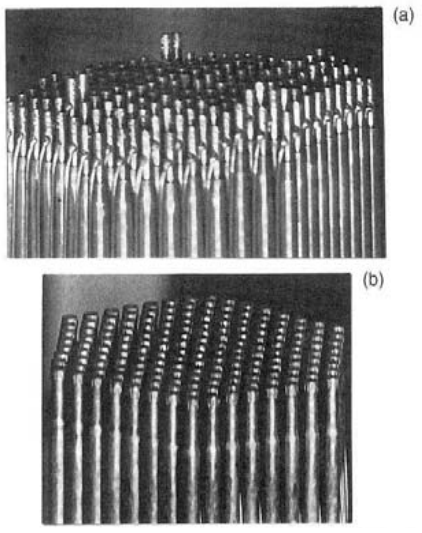

Figure.2. Dimensional changes of some of the fuel sub assembly in a reactor core (a) due to radiation damage and absence of it due to use of better material(b) in a fast reactor core.

Void Swelling: Mechanism

If the number density N_f of voids of radius R is generated in the lattice, the void swelling can be written as follows:

$$(\nabla V/V) = [(4/3)\,\pi\, R^3\,] \text{ X } N_f(R) \qquad \ldots\ldots \qquad 2.1$$

Normally, the radius of the voids is not constant and the above equation will have to take the distribution of size of voids into account while using the above equation.

The value of $\nabla V/V$ depends on many parameters, of which cumulative dose for a given operating reactor condition decides the fuel burn up. Figure.3. shows a typical variation of $\nabla V/V$ with dose, showing two regions, region 1 (transient regime) corresponding to the nucleation of stable voids and region 2 (linear regime) corresponding to steady state growth of voids. The threshold dose corresponding to ϕ_c defines the critical dose above which the material is no more recoverable or all the efforts of materials scientists is to increase the value of ϕ_c so that burn up of the fuel can be maximized.

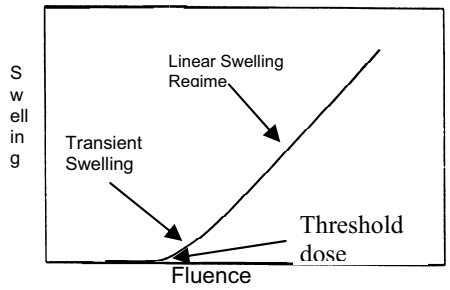

Figure.3. Schematic of variation of void swelling with dose.

The above discussions on role of void swelling on life of reactor components illustrate the importance of understanding the mechanism of void swelling and identifying the methods to combat the same.

The mechanism of void swelling is very similar to the nucleation and growth of a second phase particle in a supersaturated solid solution, if one were to consider vacancies as solutes and void as precipitate. The driving force for nucleation of voids is related to the ratio of the present concentration of vacancies to that of equilibrium concentration.

$$S = C_v \; / \; C_v^o \qquad \ldots\ldots \qquad 2.2$$

The supersaturation of vacancies is governed by thermal equilibrium concentration of vacancies in a given lattice and ease of our ability to 'knock off' an atom from its lattice position. Hence, for a given irradiation condition, a crystal at higher temperature will have less supersaturation of vacancies than the same at lower temperature. A crystal with less dissociation energy will have more 'knock ons than a lattice in which atoms are well bound and hence more concentration of vacancies. For instance, it is easy to produce more 'knock ons' in metals than in intermetallics. With respect to the energetics of the point defects, it is by now well established that it is easy to form vacancies than interstitials, as reflected by E_f^V = 0.6 to 1 eV and E_f^I = 3-4 eV. The reverse is true with respect to migration. Interstitials move faster than vacancies, due to the driving force associated with reduction of strain energy.

The theory for nucleation of voids during irradiation is an extension of similar treatment for thermal vacancies, modified by the presence of interstitials. The steady state nucleation rate of a void embryo of size n, in the presence of interstitials is set up, as follows:

$$J_n = \rho^0 (n) \; X \; \beta_V (n) \; X \; Z \quad \ldots. \qquad 2.3$$

wherein ρ^0 (n) is the concentration of voids of n vacancies, β_V (n) the rate of single vacancy impingement on a void of n vacancies and Z, the Zeldovich factor, i.e., the value of change in free energy at the critical value of radius of the voids.

The above equation has been solved to arrive at the cluster size of critical void nucleus and the radius corresponding to the same. The following trends could be deduced:

(1) Rate of nucleation of voids depends on the height of activation barrier and inclusion of interstitials raises the activation barrier and reduces the nucleation rate.

(2) The critical void radius for survival and growth as a void is a function of height of activation energy; with greater heights, requiring larger critical radius

(3) Nucleation rate is strongly increased by vacancy supersaturation and a reduced ratio of arrival rate of vacancies to interstitials.

The growth of the embryonic void depends on the rate of absorption of vacancies at its surface. But when irradiation produces equal number of vacancies and interstitials, it is expected that both the point defects are likely to arrive at the surface of the embryonic void. When an interstitial arrives, the void shrinks and it grows when vacancy arrives. Hence, the net rate of growth of voids or a steady state of growth of voids is reached depending on the balance between the absorption rate of vacancies and interstitials at the void surface. The following parameters govern the growth rate of voids:

(1) production rate of point defects during irradiation, Ko

(2) Recombination rate between a vacancy and interstitial, Kvi

(3) Rate of loss of point defects produced by various types of sinks in the matrix , Ksi, Ksv

(4) Strength of different sinks toward point defects, k_v, k_i,

(5) Diffusion rate of interstitials and vacancies, D_i, D_v and

(6) Bias term of the sinks like dislocations and voids for the point defects, z_i^d, z_v^d, z_i, and z_v.

The objective of the rate theory is to set up the void growth equation and the point defect balance equations and solve them for the growth rate of a void of radius R. The rate equations for the two types of point defects is given below:

$$dc_i/dt = K - \alpha C_i C_v - k_i^2 D_i C_i \quad \ldots. \quad 2.4$$

$$dc_v/dt = K - \alpha C_i C_v - k_v^2 D_v C_v \quad \ldots. \quad 2.5$$

wherein the subscript v and i represent the vacancies and interstitials respectively, K the recombination constant, D, the diffusion co-efficients and α, k are the constants.

The crucial factor which governs the void growth is the concentration of vacancies at the void surface, which is the net arrival of vacancies to the void. If A_{net}^V is the net arrival rate of vacancies at the void, and A_{net}^i for interstitials, D's and C's are diffusion coefficients and concentrations of the point defects and R the radius of the void, it can be shown that

$$A_{net}^V = A_v^{void} - A_i^{void} = 4 \pi R D_v (C_v - C_v^{void}) - 4 \pi R D_i (C_i - C_i^{void}) \quad \ldots.. \quad 2.6$$

The rate of growth of a void is given as follows:

$$dR/dt = (\Omega/R) [D_v (C_v - C_v^{Void}) - D_i C_i] \quad 2.7$$

wherein, Ω is the volume of defects, D and C's are diffusion co-efficients and concentrations and v and i represent vacancies and interstitials and C_v^{void} represents

the concentration of vacancies at the surface of the void. The above equation for growth rate of voids is solved for arriving at the void radius and number density of voids, from which swelling is calculated using equation 2.1.

The above simple equation, 2.7, is modified to take into consideration the real life situations like dose, dose rate and cold work. The dependence of void swelling on these factors are derived in the same way as described earlier.

Void Swelling : Dependence on dose, dose rate, temperature and dislocation density:

The variation of void swelling measured as $\nabla V/V$ vs ϕ is shown in figure.3. earlier. At low dose values, the number of vacancies and interstitials produced in a given lattice remains low. Most of these point defects generated is lost by recombination. The supersaturation is just sufficient to precipitate small voids, whose growth is inhibited by the arrival rate of vacancies at the finer voids, due to low production rate of point defects. Beyond a certain value of dose, called the threshold dose, the growth of voids increases in all systems. The rate theory calculations have been calculated for arriving at void swelling for different situations like sink dominated or recombination dominated. It is possible to show that

$$dR/dt \alpha Ko^{1/2} \quad \text{recombination dominant regions, ...} \qquad 2.8$$

$$dR/dt \alpha Ko \quad \text{sink dominated regions .....} \qquad 2.9$$

and

$$\nabla V/V (\%) = (1/4) \times (\text{dose in dpa}) \quad ..... \qquad 2.10$$

It has been shown that for most metals, the slope of the steady state growth is 1%, which does not match with the prediction of rate theory. It is possibly due to

the fact that the rate theory has not taken into consideration the presence of dislocation loops. However, the faster growth at higher dose levels is clearly due to increased supply of vacancies at the surface of the void embryos. The main attempt in the development of core component materials in fast reactors is to increase the threshold dose as high as possible.

It is necessary to understand the influence of temperature on the mechanism of void swelling before proceeding to dose rate. In the void growth equation, the highly temperature sensitive parameters are D_v and C_v^o. At low temperatures, swelling is low since D_v is low. At high temperatures, emission of vacancies by voids counterbalances the net vacancy influx by irradiation. Additionally, the supersaturation of vacancies, $S = C_v / C_v^o$ is reduced due to exponential increase in C_v^o with temperature. Hence, void swelling is low. Maximum growth rate is achieved at intermediate temperatures where both thermal emission and mutual recombinations are less important and net flow of vacancies to voids is maximized.

The influence of temperature on void swelling for a fixed combination of all other parameters like dose, dose rate and material, is shown in figure 4. It is seen that $\nabla V/V$ vs Temperature curve suggests that void swelling is less at low and high temperatures and at a suitable temperature in-between, void swelling is maximum. This can be understood as follows: At very low temperatures, the mobility of the point defects produced by irradiation is very low and hence 'recombination' is more probable than condensation into voids. At very high temperatures, the equilibrium thermal vacancy concentration increases (exponentially with temperature), reducing the driving force for condensation. Hence, emission of vacancies from the surfaces of

the voids, driven by thermodynamic requirement takes place and the void swelling is less. At a temperature in between, where these two factors are optimum, maximum swelling takes place.

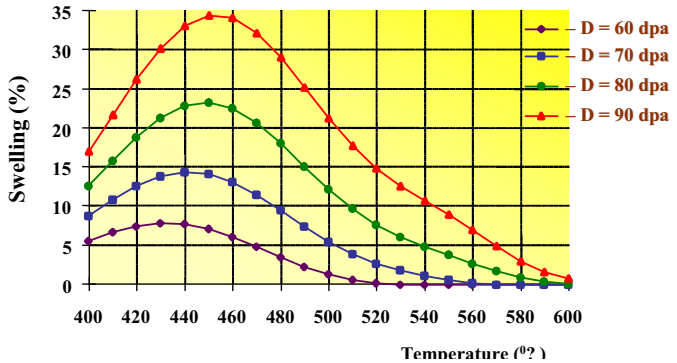

Figure.4. Dependence of swelling on irradiation temperature of steel ChS-68 of fuel pin in core of BN 600, for various dose values.

Detailed theoretical studies using rate theory has shown that the growth rate of voids is proportional to the rate of production of point defects. Effect of dose rate on void swelling can best be understood by studying the void swelling for different types of incident beams, *i.e.,* neutrons and ions. This approach is chosen mainly because of the difficulty in performing controlled reactor experiments for different dose rates with all other parameters constant. The alternate approach chosen would be sufficient for the limited purpose of comparing the mechanisms for different dose rates. The dose rate depends on two parameters: the damage cross section measured in the unit of barns (1 barn = 10^{-24} cm^2) and the flux density. Figure.8. shows that the dose rate depends on the nature of incident particle, neutron, electron or the ions. For a fixed incident energy of 1 MeV, the dose rate of heavy ions is shown to be maximum. The individual values of damage cross sections, flux density and the dose rate for each impinging particles is shown in the figure.5.

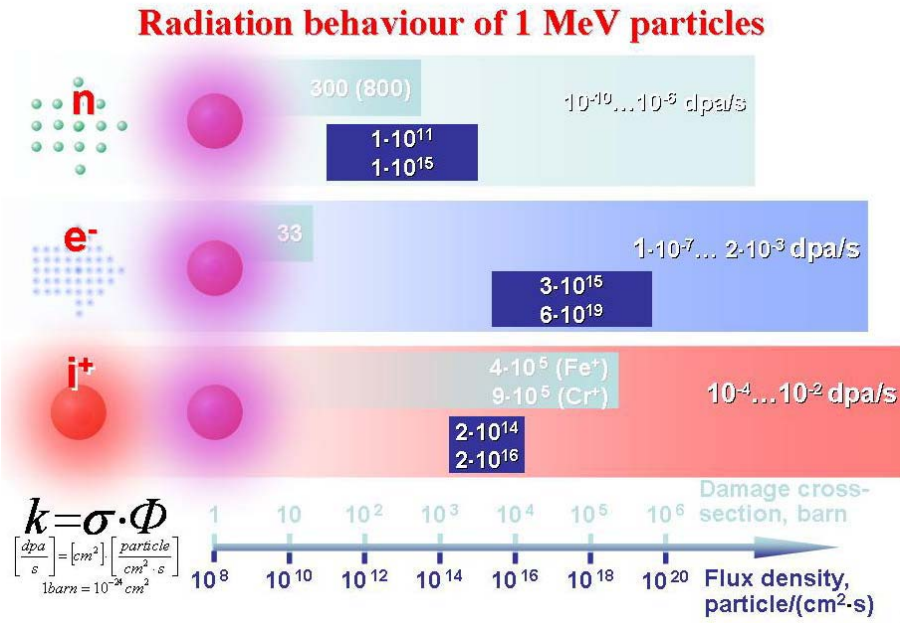

Figure.5. Variation of dose rate by changing the incident particles on the lattice. The ions produce maximum dose rate due to two orders of magnitude increase in the damage cross-sections.

The high damage rates in the case of ion irradiation as compared to neutron irradiation manifests itself in the shifting of peak of void swelling to higher temperatures as shown in Figure.6. This implies that the peak swelling temperature increases with increase in dose rate. The extent of shift in the temperature depends on the rate of damage production and the vacancy migration energy. The high damage rate in ion irradiation experiments enables screening of new materials for void swelling behaviour through reasonably fast experiments. The equivalence of the high rate damage to the much slower damage rate under neutron irradiation in a fast reactor can be expressed in terms of the temperature shift. The magnitude of this temperature shift can be written as,

$\Delta T = T_{Ni^+} - T_n = \frac{AT_{Ni^+}^2}{1 + AT_{Ni^+}}$, where T_{Ni^+} and T_n represent equivalent temperatures under Ni^+ and neutron irradiation respectively, with A, a constant representing the vacancy

migration energy, and the damage rates. Temperature shift values thus calculated can be used to determine the equivalence to neutron irradiation.

When the dose rate is high as in the case of ions, the rate of production of point defects is orders of magnitude higher. Hence, at low temperatures, the probability of recombination is high reducing void swelling. When the temperature is high enough to make the point defects mobile, supersaturation of point defects build up due to incomplete recombination and voids forms.

These information have been used in the quick screening of materials for screening of core component materials. The ion irradiation has been used to study void swelling, since it is possible to study void swelling upto high fluence levels of 100 or 200 dpa within few hours, which in a nuclear reactor, would take few years !!!

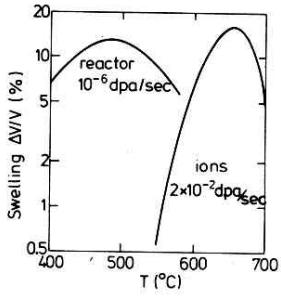

Figure.6. Shift in the ∇V/V vs Temperature curve towards higher temperature for higher dose rate of irradiation.

COLD WORK:

Cold work or the dislocation density exerts more profound influence on void swelling compared to any other parameter. The rate equation for void growth in a lattice with biased sinks as dislocations and unbiased sinks like coherent precipitates, grain boundaries is given by

$$dR_o/dt = [(K_o(Z_i-Z_v)\rho_d \Omega] / [R (Z_v \rho_d + 4\pi R \rho_v + 4\pi R_{cp} \rho_{cp})] \quad ..... \quad 2.11$$

The above equation demonstrates that both a biased sink like dislocations and neutral sinks are necessary for void growth. If $Z_i=Z_v$, i.e., the bias is removed, $dR_o/dt. = 0$, the growth rate of void is zero and no swelling occurs, since vacancies and interstitials flow equally to each sink.

Hence, to understand the relative role of strengths of biased and neutral sink, void swelling is discussed in terms of the following parameter:

Q = dislocation sink strength / void sink strength …….. 2.12

At low dose values, Q > 1 the number density of voids and their size are small. Hence, vacancy loss to existing dislocations network dominates. Hence, alloys with cold work show less swelling.

When Q=1, flow of vacancies to dislocations and voids is nearly equal. This is the regime, where the bias exerts maximum influence. If flow of vacancies and interstitials to sinks is equal and more interstitials flow to dislocations due to the bias factor, then MORE VACANCIES MUST flow to voids to maintain the point defect balance. This results in the maximum growth rate of voids.

When Q < 1, flow of defects to voids dominates the loss term. Since few defects flow to dislocations, and the bias is not effective in creating imbalances in point defect fluxes. Flow of vacancies and interstitials to voids is similar in magnitude facilitating the annihilation of the defects and void growth slows down or ceases.

Although dislocations in a cold worked material, exhibit slight preference to interstitials than vacancies, dislocations can provide high density of sinks for vacancies that effect of a vacancy supersaturation is essentially multiplied resulting in low void nucleation and growth rate of voids.

Increasing cold work reduces the amount of swelling, but at reduced rates as the amount of cold work increase. This is due to the tangling of the dislocations as the dislocation density increases, making most of the dislocation immobile and hence the preferential bias and the sink strength comes down. Primary effect of cold work is to extend “transient swelling regime” rather than to alter the steady state swelling rate.

Russian experience has shown (Figure.7.) that the void swelling reduces with increase in dislocation density only up to a certain value. That is, up to about 20% cold work, void swelling reduces and it remains constant beyond 20% cold work. The reasons for this behaviour have been explained above.

Figure.7. Effect of cold work on swelling, reaching saturation beyond 20%, a Russian experience.

To summarise, the void swelling is caused by the following process: irradiation causes point defects in the material. These point effects can either recombine or are lost to either dislocation or voids or any other sinks. Most of the point defects recombine; the dislocations in the materials exert 2% preferential bias towards interstitials, in addition to acting as effective sinks for vacancies; this leaves behind in the matrix excess vacancies,

which condense into voids when the concentration exceeds thermal equilibrium concentration value. Void swelling increases with dose very slowly in the initial stage, beyond a threshold value, increases sharply at the rate of ~ 1% per dpa for most materials. Void swelling depends on temperature, dose rate and dislocation density. The challenging job of materials designers is to increase the threshold dose for future fast reactor materials, so that higher burn-up of the fuel can be achieved.

IRRADIATION GROWTH:

As has already been explained in chapter.1, irradiation growth refers to the 'dimensional distortion' of a metal in an irradiation field, retaining the volume constant. It has been stated that a cylindrical rod of uranium, say 10 cm long 1 cm in diameter, (volume - 7.85 cm^3) irradiated to a fluence of 10^{20} n/cm^2, can increase its length three times, to 30 cm and reduce its diameter to 0.58 cm, retaining the volume same as 7.85 cm^3. The irradiation growth, anisotropic in nature, introduces severe distortion in core components. This phenomenon occurs ONLY under the influence of irradiation and stress is not present, unlike creep. Growth depends on the anisotropy of the crystal and hence occurs only in non-cubic crystals, like hcp metals of zirconium and magnesium. The models of irradiation growth suggest that the distortion is due to the condensation of interstitials preferentially as dislocation loops lying on prism planes of type (11..0) of hcp. Vacancies from as loops from the depleted zones on the basal planes (0001). This process is equivalent to transfer of atoms from the basal planes to prism planes, via irradiation induced point defects. It is obvious that in a fast reactor fuel assembly, cubic steels being the major structural alloys, irradiation growth is only of academic importance.

IRRADIATION HARDENING:

The large number density of defect loops generated during irradiation pins the mobile dislocations making them immobile. Hence, additional stress has to be applied to unpin the immobile dislocations and place them back in their glide or slip planes for free movement. This causes "*source hardening*", which is one component to the observed increase in the yield strength during irradiation. The same defect density also acts as an obstacle to the mobile dislocations, increasing the flow stress, contributing to "*friction hardening"*. Hence, a material when subjected to neutron irradiation shows 'irradiation hardening' which refers to enhanced yield strength, a smaller increase in ultimate tensile strength, a reduction in the work hardening rate ($d\sigma/d\varepsilon$, of the parabolic region) and a reduction in the uniform and total elongation. These effects are illustrated in polycrystalline copper (Figure.9.)

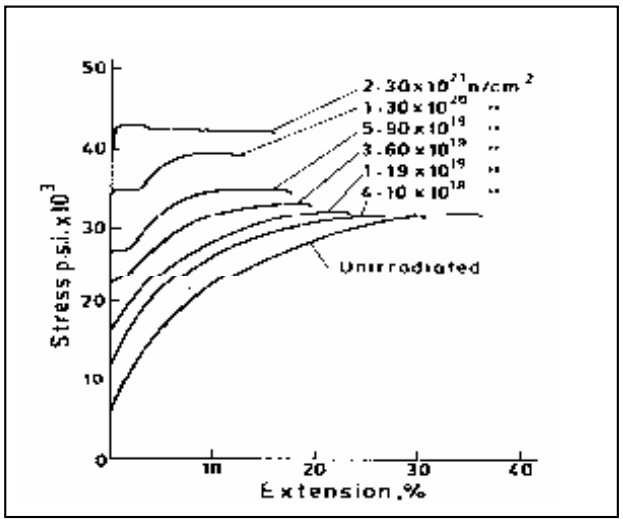

Figure. 9. Variation in stress vs strain curve for polycrystalline copper, for different irradiation dose values. Increase in stress for any given elongation and reduction in elongation with dose of irradiation is clearly observed.

A schematic picturisation of interactions of mobile dislocations with precipitates by either bowing around or cutting and pinning by voids is shown in figure.10.

According to the dispersed barrier hardening model, yield strength increases as $N^{½}$; since N, the number density of obstacle, is proportional to fluence, ϕ. The increase in yield strength due to irradiation is

$$\Delta\sigma_s^{\text{irrad.}} = (\varphi\, t)^{1/2} \quad \ldots. \qquad 2.18$$

Since number of obstacles continue to increase with dose of irradiation, $\Delta\sigma_s^{\text{irrad.}}$ is expected to continuously increase. Upto about 5 dpa, the above equation holds good in most systems, beyond which saturation in irradiation hardening is observed in many systems. At high fluence levels, the above equation is an overestimate of the irradiation hardening.

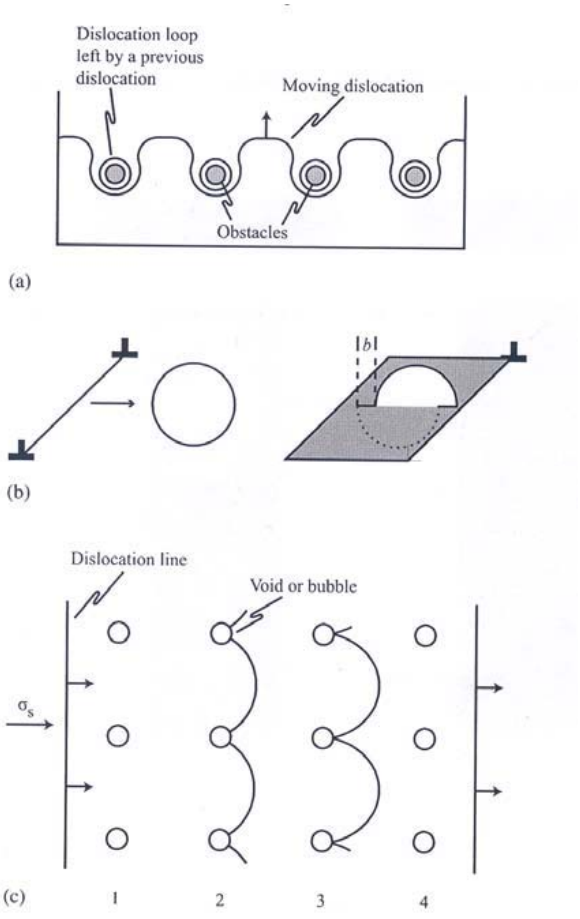

Figure.10. (a) Dislocation bowing around hard obstacles like precipitates (b) cutting and (c) interaction with voids.

Further investigations provided the possible mechanism for the observed saturation in irradiation hardening. Saturation occurs when a balance is established between creation and destruction of obstacles. Interstitial and vacancy loops are created from defect clusters. Interstitial loops grow in size as their number increases. However, vacancy loops are generally unstable and shrink by emission of vacancies. Interstitial loops are removed only by unfaulting. Hence, the calculation of number of loops should include the lifetime of the defect loops. The dispersed barrier hardening model has been modified to include the above features and found to be successful in those materials, where the hardening is basically due to dislocation loops. It was argued that once a cascade forms by the first incoming neutron, there is a certain zone around the first cascade, where the formation of subsequent defects would be reduced by the next neutron. This would ultimately reduce the number density of dislocation loops that form. This mechanism becomes more pronounced at higher doses. The equation 2.18 has been modified taking the above mechanism into effect as follows:

$$\Delta\sigma_y^{\text{irrad.}} = A\,[1 - \exp(-B\varphi\, t)]^{1/2} \quad ..... \qquad 2.19$$

where A and B are constants which depend on the volume of regions where it is difficult to produce dislocation loops because of pre-existing defects, number of such regions created per neutron collision, scattering cross-sections, in addition to the factors explained for equation 2.18.

There are some systems, where the obstacles are not only dislocation loops, but include other microstrutural features like voids or precipitates. The model has to be modified taking into consideration the type, number density and interaction strength of obstacles, to predict the irradiation hardening accurately.

The interaction between dislocations and the irradiated microstructure is mainly responsible for the reduction in rate of work hardening and ductility, in the above phenomenon of irradiation hardening. The interaction between the dislocations and the dislocation loops result in unfaulting of the loops and get incorporated into the dislocation network of the matrix. A few examples of such reactions are shown below for fcc and bcc systems:

In fcc,

$$a/2[1\text{-}1\text{-}0] + a/3\,[111] \rightarrow a/6\,[1\text{-}1\text{-}2] \quad \ldots\ldots \quad 2.20$$

$$a/6\,\{1\text{-}1\text{-}2\} + a/3\,[1\text{-}1\text{-}1\text{-}\} \rightarrow a/2\,\{110] \quad \ldots\ldots \quad 2.21$$

In bcc, faulted loops are rarely observed due to high stacking fault energy. 'unfaulting' occurs only with very small dislocation loops.

$$a/2\,[110] + a/2\,[001] \rightarrow a/2\,[111\text{-}] \text{ or} \quad \ldots. \quad 2.22$$

$$a/2\,[110] + a/2\,[11\text{-}0] \rightarrow a/2\,[010] \quad \ldots.. \quad 2.23$$

Result of each of these unfaulting reactions is the removal of dislocation loops from the microstructure and growth of dislocation network density.

The resistance to the movement of dislocations is less from dislocations than dislocation loops. Hence the rate of work hardening reduces with increase in dose, where there is reduction in the density of dislocation loops and increase in the dislocation density. The reduction in ductility also is caused by the above phenomenon of 'unfaulting' of dislocation loops. The increase in the density of dislocations causes back stresses, introducing stress raisers in the matrix. These sites act as nucleation centres for micro-cavities, initiating the non-uniform elongation region, leading to premature failure.

The application of dispersed barrier hardening model to different experimental systems showed that the model could predict the behaviour of individual alloy systems, only when the nature of obstacles to the movement of dislocations was properly accounted for. The nature of obstacle range from dislocation loops with varying density with dose, unstable matrix precipitates and stable matrix features, which include evolving metastable precipitates, voids and stable features.

IRRADIATION EMBRITTLEMENT:

Embrittlement is characterized by nearly Nil amount of plastic or creep deformation that occurs prior to fracture. Irradiation, almost always renders the materials less ductile than unirradiated condition. There are two major changes in the behaviour of materials under irradiation: (1) the Ductile to Brittle Transformation Temperature, DBTT is significantly increased due to irradiation and (2) the Upper Shelf Energy, USE is reduced considerably. A typical behaviour of materials before and after neutron irradiation is shown in the figure below:

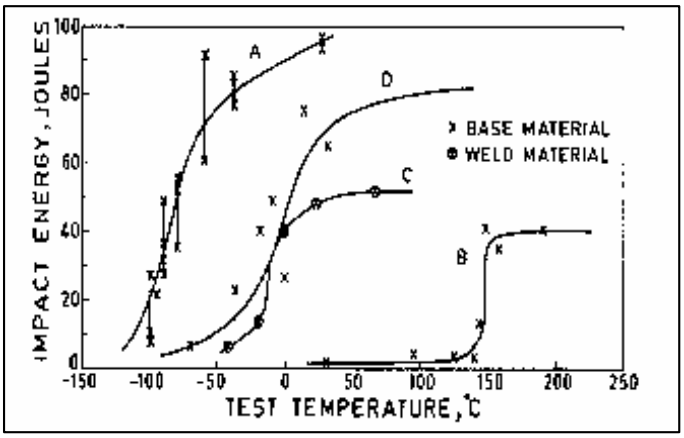

Figure.11. Variation of impact energy vs test temperature for an ASTM A 203 steel for different dose values and recovery of ductility after annealing of defects: (A) Unirradiated; (B) Irradiated to a fluence of $3.5x10^{19}$ n cm^{-2}; (C) irradiated to a fluence of $5x10^{18}$ n cm^{-2}; (D) Annealed at 300°C for 15 days after irradiation to a fluence of $3.5x10^{19}$ n cm^{-2}. Please note the increase in DBTT with dose and reduction in the upper shelf energy, with recovery of damage after annealing.

In irradiation embrittlement, the loss of ductility at lower temperatures is due to irradiation hardening discussed above and helium embrittlement at higher temperatures, which will be discussed next section.

In most basic terms, embrittlement can be understood in terms of the conditions for a crack to propagate in a material, spontaneously. Energetically, an increase in the surface area of sides of the crack is introduced, when a crack increases its length a, during a brittle failure. Energy is required to overcome the cohesive force between atoms. This is supplied by elastic strain energy which is released as the crack grows. Griffith established the following criteria for crack propagation: 'strain energy released should at least be equal to the energy required to create the new surface area'. Mathematical representation of the above condition translates into the following equation:

$$\sigma_f = 4 E \gamma_s / [(1-\nu)2 \pi c] \quad ..... \qquad 2.24$$

Wherein σ_f represents the stress required to fracture, γ_s the surface energy for creating cracks of length c and ν, the Poisson's ratio. It was realized later that there is a certain amount of plastic deformation, however small it may be, even during brittle failure, which was included in γ_s as sum of $\gamma_s + \gamma p$. Since plastic work done was found to be two orders of magnitude more than surface energy term, the equation above was simplified to

$$\sigma_f = [E \gamma_p/c]^{½} \quad ..... \qquad 2.25$$

A brittle failure has three stages:

(1) plastic deformation, resulting in pile of dislocations along the slip plane at an obstacle;

(2) build up of shear stress ahead of pile up, nucleating a crack and

(3) propagation of crack, where the stored strain energy drives the micro-cracks to create fresh surface, converting the strain energy to surface energy.

The first part , the plastic deformation is treated using theory of yielding, i.e., the Hall-Petch relation:

$$\sigma_y = \sigma_0 + k [d]^{-½} \quad \ldots\ldots\ldots \quad 2.26$$

The first term in the above equation refers to the friction hardening contribution, while the second terms represents the source hardening. Materials with high k value, i.e., those which release more dislocations into the system, when a source is unlocked, like ferritics, are more prone to brittle failure. In bcc metals, σ_0 the friction hardening terms increases rapidly as temperature decreases below room temperature and leads to more brittle behaviour than others.

During irradiation, copious amount of defects clusters are produced. These increase the frictional component of yield strength, by increasing the resistance to movement of dislocations. Increase in yield strength due to irradiation, displaces the temperature at which brittle fracture appears to higher temperatures (Figure.12.) Drastic loss in ductility at low temperatures results from different sensitivity of σ_f and σ_y to neutron damage. σ_f is not significantly influenced by irradiation and less dependent on temperature than σ_y. The DBTT is given by the condition that σ_f must be equal to σ_y The temperature at which the two stresses become equal is given by

$$T_c = C^{-1} [\ln B k_s d^{1/2} / (\beta\gamma\mu - k_y k_s) \quad \ldots\ldots \quad 2.27$$

Wherein B and C are constants, d, the grain size, k_y k_s are Petch slope and irradiation induced increase in yield strength, β, a constant related to the degree of triaxiality of

stress around the crack, γ effective surface energy (including plastic)and μ, the shear modulus

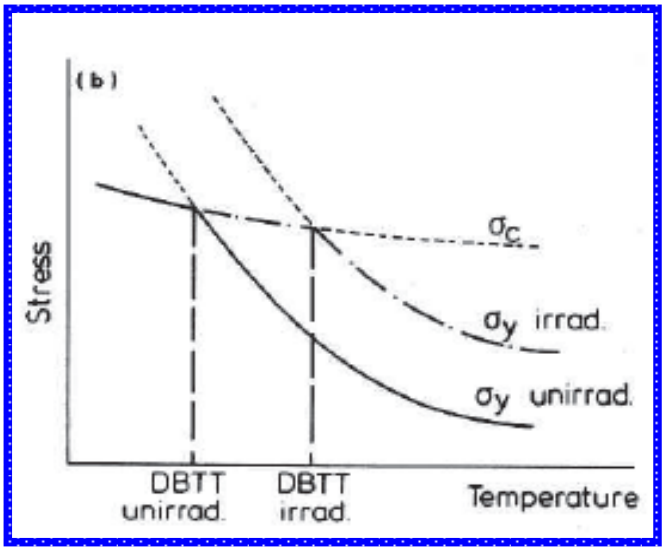

Figure.12. Irradiation Embrittlement: Shift in DBTT as a result of difference in the sensitivity of yield strength and fracture strength with temperature. The increase in DBTT is only a consequence of irradiation hardening, as seen by the higher yield strength for irradiated materials.

Irradiation induced segregation of embrittling elements like phosphorous, antimony and tin, called 'metalloids', reduces fracture stress, causing additional shift in DBTT.

Irradiation embrittlement not only increases DBTT, but also reduces the upper shelf energy, which also is a consequence of increased yield strength due to irradiation. The change in the upper shelf energy is given as follows:

$$f = k \Delta\sigma_y \text{ for smaller changes ....} \qquad 2.28$$

and of the form

$$f = k \Delta\sigma_y + \sqrt{(P \Delta\sigma_y - Q)}, \text{ for larger change,} \qquad 2.29$$

where P and Q are constants.

To summarise, it can be stated that the irradiation embrittlement is caused by

(1) irradiation hardening increasing the yield strength;

(2) increase in k i.e., number of dislocations that are released in a pile up when a source is unlocked and

(3) decrease in effective surface energy due to impurities.

HELIUM EMBRITTLEMENT:

At high temperature, the nature of fracture gets changed to predominantly grain boundary assisted intergranular failure. This is in contrast to transgranular failure at low temperatures. At high temperatures, the relative strength of grain boundary to that of matrix is reduced, as a result of grain boundary sliding, wedge cracking near triple points, formation of brittle, continuous secondary phases or voids or bubbles along grain boundary. These processes reduce the time to failure, t_f drastically, which has inverse relation with area fraction of grain boundary cavities. During irradiation, some of the structural elements like nickel undergo (n,α) reactions, resulting in copious production of helium atoms. The binding energy of helium with vacancy being very high ~ 2 eV, the helium atoms stabilize the voids and enables them to grow bigger. Incorporation of helium during irradiation into voids along the grain boundary assist grain boundary crack growth by link up of voids. In normal metals, high temperature grain boundary embrittlement is characterized fracture along grain boundaries. Irradiation during deformation enhance the processes, leading to significant reduction in the time to failure.

IRRADIATION CREEP:

Irradiation creep is the parameter of most importance, next only to void swelling, since this forms one of the design parameters. If a material is exposed to stress below the yield or ultimate tensile stress, at high temperatures, for a prolonged duration of six

months or sometimes even more, permanent deformation of the material, leading eventually to fracture. This phenomenon is understood as “creep” caused by thermally activated deformation mechanisms. Normally, the material undergoes three stages (Figure.13a) of creep: the primary creep during which strain hardening takes place, the secondary creep where the hardening due to the external stress is off-set by the recovery caused by thermal energy, followed finally by the tertiary stage where exponential increase of strain rate is observed leading to final fracture. The nucleation of disconnected cracks in the end of the second stage and their linkages in the tertiary stage cause the fracture, as shown in figure.13a. The stress-strain or the creep behaviour of a material depends normally on the externally applied stress and the temperature, as shown in figure 13 b and c.

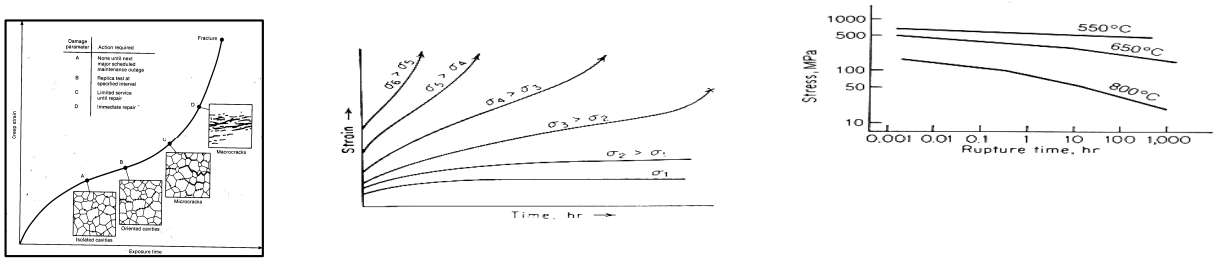

Figure.13. Creep Behaviour of Materials: a) Three stages in a creep curve; b) Effect of external stress on the creep curves and c) Effect of temperature on creep curves

When irradiation is superimposed on external stress and temperature, the material undergoes irradiation creep, which refers to ‘augmentation’ of thermal creep and termed as “irradiation enhanced creep”. Under certain combination of external stress and temperature, material may not display thermal creep. However, if irradiation is superimposed, material develops creep conditions, which is termed as irradiation induced creep. Figure.14. shows the ratio of change in diameter to original diameter, *i.e.,*

diametral strain with fluence or dose to which 20% cold worked austenitic stainless steel was exposed in EBR-II reactor for various values of hoop stress.

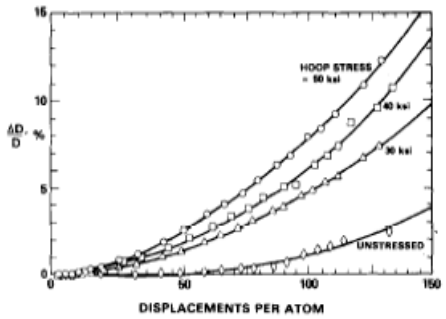

Figure.14. Diameter changes in 20 % cold worked 316 austenitic stainless steels after irradiation in EBR-II for different hoop stress levels.

The irradiation creep illustrated in the figure above is influenced by the temperature very strongly. At $T < 0.3\ T_m$, reduction in creep rate is observed, under irradiation. This temperature range refers to the regime where dislocation glide along its slip planes is active. But the matrix in which dislocations need to glide is hardened by the irradiation induced defect clusters. Hence, creep rate reduces.

At $T > 0.3$ Tm, irradiation increases creep rate. It is known that at these temperatures, climb controlled glide is the operative mechanism and the excess vacancies introduced by irradiation assist glide, increasing the creep rate.

At $T > 0.6$ Tm, the concentration of vacancies introduced by irradiation is less than at thermal equilibrium. Hence, irradiation loses its influence and thermal creep would be dominant.

Irradiation creep also depends on the dose values, at a constant temperature. Most often, irradiation creep occurs simultaneously with swelling and most often, swelling influences irradiation creep. At very small dose levels, swelling enhances creep rates.

Beyond a certain dose levels, creep component reduces and at high dose levels, creep disappears, while swelling continues. Figure. 15. shows the variation in creep co-efficient at various dose levels, and the regimes where swelling has an influence.

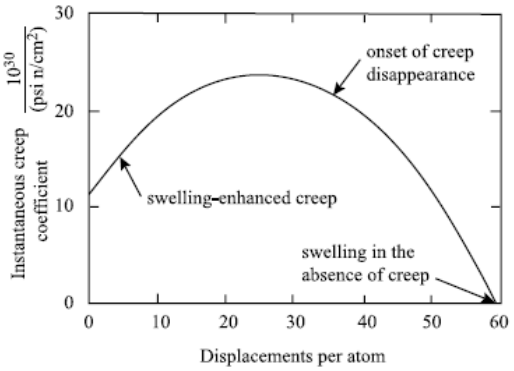

Figure.15. Schematic to demonstrate the influence of swelling in creep rate for increasing dose values.

The dynamics of point defects during irradiation continuously evolves with change in structure of dislocation network and loops. At small dose levels, there is a uniform distribution of very fine voids, which act as effective pinning centers for mobile dislocations. Thus the creep rate increases. With increase in dose levels, voids grow and multiply. The chance of interstitials and vacancies impinging on the void surface becomes more than their reaching dislocations. The number of interstitials reaching a dislocation reduces. Additionally, the defect clusters, i.e., the dislocation loops also undergo ‘faulting’ contributing to the density of dislocations in the matrix. Hence, creep rate reduces, due to two factors: increased dislocation density of the matrix due to unfaulting of dislocation loops and reduced availability of interstitials to dislocations. The above process continues till complete cessation of creep, with swelling continuing to take place.

Numerous mechanisms have been identified to understand the irradiation creep, all of which revolve around the excess point defects generated during irradiation and their interaction with dislocations. One of the accepted mechanisms (Figure.16.) is based on pure dislocation climb process, termed as "Stress Induced Preferential Absorption" (SIPA) of point defects by dislocations. This mechanism can be understood as due to two reasons: (1) When a matrix consists of random distribution of dislocations and point defects, there is a net excess flow of interstitials to dislocations whose extra half planes are perpendicular to the stress axis. This preferential flow is due to the minimization of strain energy. Similarly, the excess vacancies flow to dislocations with other configurations. Effectively, this preferential flow of interstitials, create more new planes of atoms nearly perpendicular to the stress axis. (2) Creep is caused by dislocation glide, enabled by dislocation climb. During irradiation, excess interstitials are attracted towards dislocations of all orientations, (see void swelling), causing climb-enabled glide.

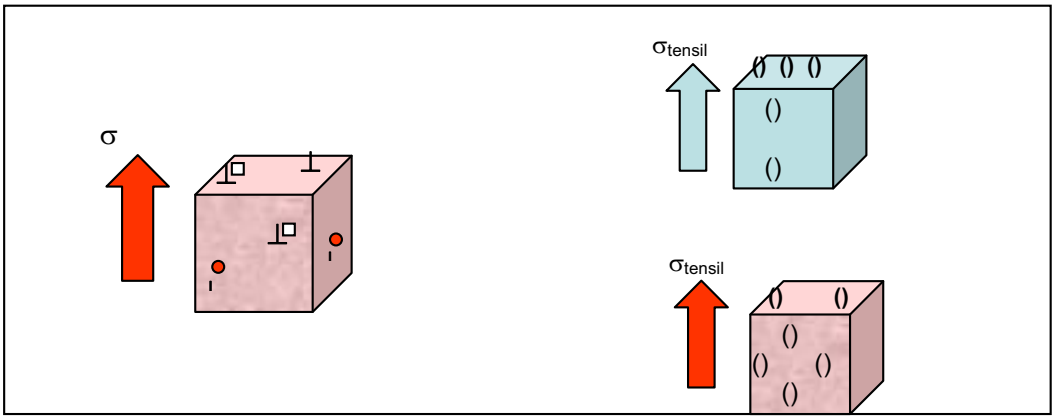

Figure.16. Mechanisms of SIPA and SIPN.

There is yet another mechanism describing irradiation creep called the "Stress Induced Preferential Nucleation –SIPN". This is understood based on the preferential

nucleation of dislocation loops of either vacancies or interstitials produced by irradiation. When the external stress is high, the interstitial loops form preferentially in planes perpendicular to the tensile axis. The same occurs for vacancy loops at low values of external stress. The net effect is similar to that of SIPA, resulting in preferential extra planes.

At very high temperatures, the point defect migration along the grain boundaries, in preferential routes cause the grain boundary aided creep. The mechanism is illustrated in the figure 17. Finally, the effect of irradiation creep is to increase the diameteral strain with increase in dose, leading to premature failure.

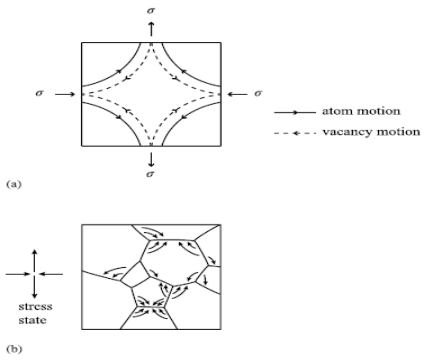

Figure.17. Migration of point defects at high temperatures to prefentially oriented grain boundaries, as in thermal creep augmented by excess point defects in irradiation creep.

SUMMARY:

The various phenomena that has been introduced separately, very often takes place simultaneously. These phenomena are also influenced by the physical changes described in chapter 1, as segregation and phase stability. There is a favourable combination of radiation dose and temperature that augments certain damage mechanisms. Such features are compiled together for a typical ferritic steel and presented in figure.18, much along the same lines as deformation maps or Ashby's fracture mechanism maps. It is seen that for most practical purposes, in the pertaining temperature

range where fast reactors operate, hardening, irradiation creep and void swelling are dominant. The void swelling and the irradiation creep are the major factors which govern the choice of materials for core components in a fast breeder reactor. Embrittlement sets in even at low dose and temperature, which at higher dose levels is replaced by helium mebrittlement and a shift in DBTT. At high temperatures, softening domains exists for the present generation steels. There is a significant reduction in the creep strain to about 1 or 2 % at high temperatures and at high dose levels. This loss of creep life, due to irradiation creep mechanisms is the major life limiting factor for fast reactor materials. Hence, the high temperature limit presently is restricted to about 550 C. Materials technologists are making their best efforts to enhance this limit to 600 or 700 C. This could probably be the maximum temperature that can be achieved with present generation steels, for the medium temperature fast reactors.

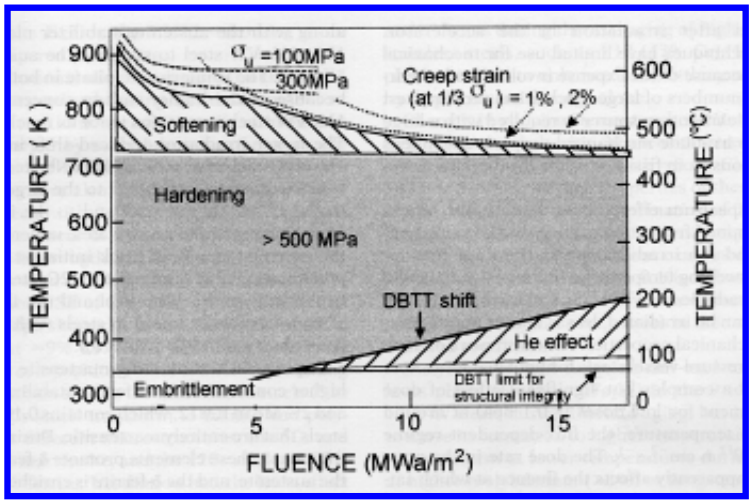

Figure.18. Summary of Radiation Damage Mechanisms in ferritic steels, in a fast reactor fuel assembly, for various combinations of fluence i.e. irradiation dose and temperature.